Progress In Electromagnetics Research M, Vol. 112, 115–125, 2022

A 2-D DOA Estimation Algorithm for L-Shaped Array with Improved Computational Efficiency

Jie Yang and Hu He*

Abstract—A high-precision and high-efficiency reduced-dimension direction of arrival (DOA) estimation algorithm based on an L-shaped array for the problems of large computation and high cost of achieving two-dimensional (2D) DOA estimation by 2D multiple signal classification (MUSIC) algorithm under various complex arrays. The algorithm makes full use of the structural characteristics of the L-shaped array to decompose the uniform L-shaped array into two uniform linear arrays. These two arrays are respectively searched in one-dimension (1D) to estimate the angles between the source and the x-axis and y-axis, and then the 2D DOA estimation is obtained according to the geometric relationship, which greatly reduces the amount of computation. Furthermore, the algorithm increases the utilization of noise subspace information, which not only realizes the automatic pairing of direction angle and elevation angle, but also improves the estimation accuracy. In order to further reduce the complexity and improve the estimation performance, this paper also puts forward the root finding method instead of 1D search and uses a fast angle matching method to accurately match angles. Simulation results show the feasibility of the proposed algorithm.

1. INTRODUCTION

Direction of arrival (DOA) estimation has always been one of the hot topics in array signal processing. It is widely used in radar, sonar, medical diagnosis, wireless communication, and other fields [1–4], which has great research significance. In recent decades, many super-resolution DOA estimation algorithms have been proposed, including the famous multiple signal classification (MUSIC) algorithm [5] and estimating of signal parameter via rotational invariance techniques (ESPRIT) [6]. Early research on these algorithms mostly stayed in one-dimensional (1D) array. Since 1D DOA estimation can only provide 1D estimation information of incident wave, there are many defects in practical application, so more and more researchers are engaged in the research of two-dimensional (2D) DOA estimation [7–22]. Among these research results, the 2D-MUSIC algorithm is one of the most classic algorithms in current 2D-DOA estimation research. This method can generate asymptotically unbiased estimation with high accuracy and flexibility [7]. However, it needs to search for spectral peaks in 2D space, which is extremely computationally intensive and difficult to meet the needs of practical application. The complexity of this algorithm mainly focuses on two parts: eigenvalue decomposition (EVD) to obtain subspace and 2D spectral peak search to obtain direction angle estimation. Thus, in order to reduce the computational complexity, many algorithms use more concise methods to equate these two modules, such as: Wu et al. [8] proposed a 2D propagator method (PM) algorithm without EVD. Strobach [9] proposed a 2D ESPRIT algorithm without searching for spectral peaks. There are also some algorithms to reduce the complexity of the algorithm by reducing the dimension of the 2D DOA estimation algorithm [10–13], that is, using corresponding mathematical knowledge to simplify the 2D problem to the 1D level for

Received 16 April 2022, Accepted 24 June 2022, Scheduled 28 July 2022
* Corresponding author: Hu He (1145562798@qq.com).
The authors are with the School of Communication and Information Engineering, Xi'an University of Posts and Telecommunications, Xi'an 710121, China.

processing. This way can also effectively improve the running speed of the algorithm. Although the above algorithm has a great improvement in the calculation speed, complex array structure, difficult implementation, and high cost in practical applications are not conducive to practical promotion.

Different from the single structure of a 1D DOA estimation array, the structure of a 2D DOA estimation array is diverse and has an important impact on the estimation results. Among many array structures, L-shaped array has attracted more and more attention due to its simple structure, easy implementation, excellent estimation performance, and small Cramer-Rao bound (CRB) [14–16]. In the research on L-shaped arrays, a PM algorithm using one or two L-shaped arrays is proposed in [17]. This algorithm solves the problem that the PM algorithm needs angle pairing under parallel arrays, and the estimation will fail when the elevation angle is between 70° and 90°. However, this algorithm has errors in the pairing of elevation angle and azimuth angle [18], and it was more difficult to implement because it needed multiple arrays. In [19], a 2D DOA estimation method that can automatically perform angle matching is proposed. A new steering vector is calculated by introducing synthetic angle, and then the azimuth and elevation angles of the source are calculated. However, the algorithm needs multiple angle search and EVD, which leads to the high complexity of the algorithm. Ref. [20] makes full use of the cross-correlation information of x-axis and z-axis subarray received data to suppress the background noise, thereby significantly enhancing the performance of DOA estimation. But the algorithm must rely on a large enough number of snapshots. Ref. [21] proposed a reduced complexity MUSIC (RC-MUSIC) algorithm based on unfolding coprime L-shaped array. This algorithm uses the cross-correlation information of the received signals between two subarrays to convert the 2D peak search into 1D search, which reduces the complexity of 2D-MUSIC algorithm, increases the array aperture, and improves the estimation accuracy. However, when searching the 1D spectral peak, this algorithm only uses a part of the total noise subspace as the noise subspace of the x-axis subarray. It limits the further improvement of estimation accuracy. Like the algorithm proposed in [22], in order not to do extra angle matching work, it is necessary to repeatedly search for spectral peaks, which increases the complexity of the algorithm.

Based on the above analysis, the algorithm proposed in this paper makes full use of the particularity of L-shaped array structure. And the 2D DOA estimation is converted into two 1D DOA estimates by dimension reduction without quadratic optimization. The algorithm takes full advantage of the covariance information of the whole array to construct the noise subspace, which reduces the algorithm complexity and improves the estimation accuracy. Compared with 2D-MUSIC algorithm, the complexity of the algorithm after dimension reduction has been greatly cut down. On this basis, using root-finding method instead of 1D peak search can further improve the calculation speed and estimation accuracy of the algorithm. Finally, the simulation experiment shows the effectiveness and practicability of the proposed algorithm.

2. SIGNAL MODEL

The structure of L-shaped uniform array is shown in Fig. 1(a). There are M sensors ($2M-1$ sensors in total) on the x-axis and y-axis, respectively, and the sensor spacing is $d = \lambda/2$, where λ is the signal wavelength. Suppose that there are K ($K < 2M-1$) independent far-field narrow-band signals, incident on the array plane at a 2D angle (θ_k, ϕ_k) $(k = 1, 2, \cdots, K)$; θ_k and ϕ_k are the azimuth and elevation angles of the kth incident source; $\theta_k \in [0, 90°]$, $\phi_k \in [0, 90°]$. α_k and β_k are the included angles between the kth target signal and x-axis and y-axis respectively, where $\alpha_k \in [0, 90°]$, $\beta_k \in [0, 90°]$, as shown in Fig. 1(b).

With the sensor at the origin as the reference point, the signal models received by x-axis and y-axis can be expressed as

$$\mathbf{x}(t) = \mathbf{A}_x(\theta, \phi)\mathbf{S}(t) + \mathbf{N}_x(t) \tag{1}$$

$$\mathbf{y}(t) = \mathbf{A}_y(\theta, \phi)\mathbf{S}(t) + \mathbf{N}_y(t) \tag{2}$$

where $\mathbf{A}_x(\theta, \phi) = [\mathbf{a}_x(\theta_1, \phi_1), \cdots, \mathbf{a}_x(\theta_K, \phi_K)]$ is the manifold matrix of x-axis array, and similarly, $\mathbf{A}_y(\theta, \phi) = [\mathbf{a}_y(\theta_1, \phi_1), \cdots, \mathbf{a}_y(\theta_K, \phi_K)]$ is the manifold matrix of y-axis array. $\mathbf{S}(t) = [\mathbf{S}_1(t), \mathbf{S}_2(t), \cdots, \mathbf{S}_K(t)]^T$ is a complex source matrix, and $\mathbf{S}(t) \in \mathbf{C}^{K \times L}$, where L represents the number of sampling points. $\mathbf{N}_x \in \mathbf{C}^{M \times L}$ and $\mathbf{N}_y \in \mathbf{C}^{M \times L}$ are the complex vectors of noise received by the

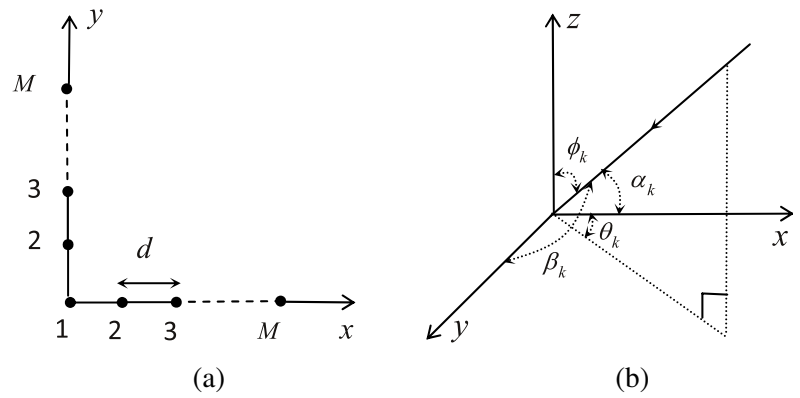

Figure 1. System model. (a) L-shaped uniform array, (b) signal incident on antenna array.

x-axis and y-axis arrays respectively. It is assumed that the noise received by each sensor is additive Gaussian white noise with the mean value of 0 and variance of σ^2. Also the noise is irrelevant to the source $\mathbf{S}(t)$.

The steering vector of the kth target source is defined as

$$\mathbf{a}_x(\theta_k, \phi_k) = \left[1, \exp\left(\frac{w_1}{d}\right), \cdots, \exp\left(\frac{w_{M-1}}{d}\right)\right]^T \tag{3}$$

$$\mathbf{a}_y(\theta_k, \phi_k) = \left[1, \exp\left(\frac{p_1}{d}\right), \cdots, \exp\left(\frac{p_{M-1}}{d}\right)\right]^T \tag{4}$$

where $w_m = j2\pi m \cos\theta_k \sin\phi_k$, $m = 1, \cdots, M-1$, $p_m = j2\pi m \sin\theta_k \sin\phi_k$, $m = 1, \cdots, M-2$.

Combining $\mathbf{x}(t)$ and $\mathbf{y}(t)$, the received signal matrix can be constructed as

$$\mathbf{z}(t) = \begin{bmatrix} \mathbf{x}(t) \\ \mathbf{y}(t) \end{bmatrix} = \mathbf{A}(\theta, \phi)\mathbf{S}(t) + \mathbf{N}(t) = \begin{bmatrix} \mathbf{A}_x(\theta, \phi) \\ \mathbf{A}_y(\theta, \phi) \end{bmatrix} \mathbf{S}(t) + \begin{bmatrix} \mathbf{N}_x(t) \\ \mathbf{N}_y(t) \end{bmatrix} \tag{5}$$

the covariance matrix $\mathbf{R}$ of $\mathbf{z}(t)$ can be expressed as

$$\mathbf{R} = E(\mathbf{z}(t)\mathbf{z}(t)^H) = \mathbf{A}(\theta, \phi)\mathbf{R}_S\mathbf{A}^H(\theta, \phi) + \mathbf{R}_N \tag{6}$$

Since the sources are independent of each other, the source covariance matrix $\mathbf{R}$ is non-singular, where $\mathbf{R}_N = \sigma^2\mathbf{I}$ is the noise covariance matrix, and $\mathbf{I} \in \mathbf{C}^{(2M-1)\times L}$ is the identity matrix.

$\mathbf{R}$ is known as Hermite matrix, and its EVD can be expressed as

$$\mathbf{R} = \begin{bmatrix} \mathbf{U}_S & \mathbf{U}_N \end{bmatrix} \mathbf{\Lambda} \begin{bmatrix} \mathbf{U}_S^H \\ \mathbf{U}_N^H \end{bmatrix} \tag{7}$$

where $\mathbf{U}_S$ is a signal subspace composed of eigenvectors corresponding to K large eigenvalues. Correspondingly, $\mathbf{U}_N$ is a noise subspace composed of eigenvectors corresponding to $2M - K - 1$ small eigenvalues. $\mathbf{\Lambda}$ is a diagonal matrix composed of eigenvalues.

It should be noted that in practical application, the covariance matrix of the signal is approximated by its sampling covariance matrix as

$$\hat{\mathbf{R}} = \frac{1}{L}\sum_{l=1}^{L} \mathbf{z}(t_l)\mathbf{z}^H(t_l) \tag{8}$$

It is known that under ideal conditions, the signal subspace and noise subspace are orthogonal to each other [5], so Eq. (9) can be obtained by simultaneously right multiplying $\mathbf{U}_N$ on both sides of the equal sign of (7)

$$\mathbf{R}\mathbf{U}_N = \begin{bmatrix} \mathbf{U}_S & \mathbf{U}_N \end{bmatrix} \mathbf{\Lambda} \begin{bmatrix} \mathbf{0} \\ \mathbf{I} \end{bmatrix} = \sigma^2\mathbf{U}_N \tag{9}$$

in combination with (6), (7), and (9), the following equation can be constructed

$$\mathbf{R}\mathbf{U}_N = \mathbf{A}(\theta,\phi)\mathbf{R}_S\mathbf{A}^H(\theta,\phi)\mathbf{U}_N + \sigma^2\mathbf{U}_N = \sigma^2\mathbf{U}_N \tag{10}$$

simplify (10) to

$$\mathbf{A}(\theta,\phi)\mathbf{R}_S\mathbf{A}^H(\theta,\phi)\mathbf{U}_N = \mathbf{0} \tag{11}$$

Since $\mathbf{R}_s$ is a non-singular matrix, that is, the determinant is not equal to zero, we can deduce $\mathbf{A}^H(\theta,\phi)\mathbf{U}_N = \mathbf{0}$, which indicates that each column vector of matrix $\mathbf{A}(\theta,\phi)$ is orthogonal to the noise subspace

$$\mathbf{U}_N^H\mathbf{a}(\theta_i,\phi_i) = \mathbf{0} \quad i = 1,2,\cdots,K \tag{12}$$

through the above derivation, the spatial spectral function of 2D MUSIC algorithm can be denoted as

$$P_{\text{2D-MUSIC}}(\theta,\phi) = \frac{1}{\mathbf{a}^H(\theta,\phi)\mathbf{U}_N\mathbf{U}_N^H\mathbf{a}(\theta,\phi)} \tag{13}$$

where $\mathbf{a}(\theta,\phi) = [\mathbf{a}_x^T(\theta,\phi), \mathbf{a}_y^T(\theta,\phi)]^T$, and K target signals can be obtained by performing a 2D spectral peak search on (13).

3. IMPROVED DOA ESTIMATION METHODS

The classical 2D-MUSIC algorithm requires complex 2D spectral peak search. It also makes insufficient use of the noise subspace information of the whole array. Therefore, in this section, firstly, a reduced-dimension (RD) MUSIC algorithm is proposed to reduce the complexity and improve the estimation accuracy. Instead of 1D search, a root-finding algorithm is proposed to further reduce the algorithm complexity.

3.1. Proposed RD-MUSIC Algorithm

Among many 2D DOA estimation arrays, due to the particularity of the L-shaped array structure, it can be decomposed into two uniform linear arrays on the basis of its array structure. 1D DOA estimation is performed on α_k and β_k, respectively. As can be seen from the geometric relationship shown in Fig. 1(b)

$$\begin{cases} u_k = \cos\alpha_k = \cos\theta_k\sin\phi_k \\ v_k = \cos\beta_k = \sin\theta_k\sin\phi_k \end{cases} \tag{14}$$

the estimated value of u_k is obtained by using the received signal of the sensor on the x-axis; the estimated value of v_k is obtained by using the received signal of the sensor on the y-axis.

The steering vector represented by (3) and (4) can be rewritten as

$$\mathbf{a}(u_k) = \left[1, \exp\left(\frac{w_1}{d}\right), \cdots, \exp\left(\frac{w_{M-1}}{d}\right)\right]^T \tag{15}$$

$$\mathbf{a}(v_k) = \left[1, \exp\left(\frac{p_1}{d}\right), \cdots, \exp\left(\frac{p_{M-1}}{d}\right)\right]^T \tag{16}$$

then the manifold matrices of the array on the x-axis and y-axis are $\mathbf{A}(u) = [\mathbf{a}(u_1),\cdots,\mathbf{a}(u_K)]$ and $\mathbf{A}(v) = [\mathbf{a}(v_1),\cdots,\mathbf{a}(v_K)]$, respectively.

X-axis and y-axis array covariance matrices $\mathbf{R}_X$ and $\mathbf{R}_Y$ can be decomposed into two spaces, namely

$$\mathbf{R}_X = \mathbf{U}_{X_S}\mathbf{\Sigma}_{X_S}\mathbf{U}_{X_S}^H + \mathbf{U}_{X_N}\mathbf{\Sigma}_{X_N}\mathbf{U}_{X_N}^H \tag{17}$$

$$\mathbf{R}_Y = \mathbf{U}_{Y_S}\mathbf{\Sigma}_{Y_S}\mathbf{U}_{Y_S}^H + \mathbf{U}_{Y_N}\mathbf{\Sigma}_{Y_N}\mathbf{U}_{Y_N}^H \tag{18}$$

where $\mathbf{\Sigma}_{X_S}$ and $\mathbf{\Sigma}_{Y_S}$ are diagonal matrices composed of K large eigenvalues of $\mathbf{R}_X$ and $\mathbf{R}_Y$, respectively; $\mathbf{\Sigma}_{X_N}$ and $\mathbf{\Sigma}_{Y_N}$ are diagonal matrices composed of $M-K$ small eigenvalues of $\mathbf{R}_X$ and $\mathbf{R}_Y$, respectively.

From the orthogonal relationship between noise eigenvector and signal direction vector, the following array spatial spectral function can be obtained

$$f(u) = \frac{1}{\mathbf{a}^H(u)\mathbf{U}_{X_N}\mathbf{U}_{X_N}^H\mathbf{a}(u)}, \quad u \in (0,1) \tag{19}$$

and the estimated value $\hat{u}_k\,(k=1,2,\cdots,K)$ of u_k can be obtained through spectral peak search. Then put $\mathbf{a}(\hat{u}_k)$ as a constraint condition into the following spatial spectral function, the estimated value $\hat{v}_k$ of v_k corresponding to $\hat{u}_k$ can be obtained

$$f(v)=\frac{1}{\begin{bmatrix}\mathbf{a}(\hat{u}_k)\\ \mathbf{a}(v)\end{bmatrix}^H\mathbf{U}_N\mathbf{U}_N^H\begin{bmatrix}\mathbf{a}(\hat{u}_k)\\ \mathbf{a}(v)\end{bmatrix}},\quad v\in(0,1) \tag{20}$$

Obtain the automatically paired $\hat{u}_k$ and $\hat{v}_k$ through (19) and (20), then the estimated values of the azimuth and elevation angles can be expressed as

$$\hat{\theta}_k = \arctan(\hat{v}_k/\hat{u}_k) \tag{21}$$

$$\hat{\phi}_k = \arcsin(u_k^2+v_k^2)^{1/2} \tag{22}$$

3.2. Proposed Root-RD-MUSIC Algorithm

The above method still needs to perform 1D search, and the specific calculation amount is related to the search accuracy. Therefore, in order to further improve the estimation speed, the root-finding method with less calculation can be used to replace the search method.

Combining (14), define

$$\begin{cases} z_1=\exp(j2\pi d\cos\alpha/\lambda)\\ z_2=\exp(j2\pi d\cos\beta/\lambda)\end{cases} \tag{23}$$

and the steering vector can be rewritten as

$$\mathbf{a}(\alpha) = \left[1,z_1,\cdots,z_1^{M-1}\right]^T=\mathbf{a}(z_1) \tag{24}$$

$$\mathbf{a}(\beta) = \left[1,z_2,\cdots,z_2^{M-1}\right]^T=\mathbf{a}(z_2) \tag{25}$$

the zeros of the denominator in the spectral peak search function can be found by using the orthogonality of the noise eigenvector and the signal steering vector. To eliminate α and β, one can replace $\mathbf{a}^H(\alpha)$ with $z_1^{M-1}\mathbf{a}^T(z_1^{-1})$ and $\mathbf{a}^H(\beta)$ with $z_2^{M-1}\mathbf{a}^T(z_2^{-1})$, i.e.,

$$f(z_1) = z_1^{M-1}\mathbf{a}^T(z_1^{-1})\mathbf{U}_{X_N}\mathbf{U}_{X_N}^H\mathbf{a}(z_1)=0 \tag{26}$$

$$f(z_2) = z_2^{M-1}\mathbf{a}^T(z_2^{-1})\mathbf{U}_{Y_N}\mathbf{U}_{Y_N}^H\mathbf{a}(z_2)=0 \tag{27}$$

where $f(z_1)$ and $f(z_2)$ are polynomials of degree $2(M-1)$, that is, they each has $M-1$ pairs of roots, and each pair of roots is mirror symmetry (conjugate symmetry) with respect to the unit circle. Theoretically, K roots are just distributed on the unit circle. In practice, due to the influence of noise and other factors, solve Equations (26) and (27), and take the K roots $\hat{\mathbf{z}}_1=[\hat{z}_{11},\hat{z}_{12},\cdots,\hat{z}_{1K}]$ and $\hat{\mathbf{z}}_2=[\hat{z}_{21},\hat{z}_{22},\cdots,\hat{z}_{2K}]$ whose absolute values are closest to the unit circle, respectively, so as to obtain the estimates of $\cos\alpha_k$ and $\cos\beta_k$

$$\cos\hat{\alpha}_k = \text{angle}(\hat{z}_{1k})/2\pi d \tag{28}$$

$$\cos\hat{\beta}_k = \text{angle}(\hat{z}_{2k})/2\pi d \tag{29}$$

Since the estimates of α_k and β_k are obtained from the x and y axes, respectively, the corresponding $\hat{\alpha}_k$ and $\hat{\beta}_k$ need to be paired. In this regard, the maximum likelihood estimation method is used in this paper, and the cost function is defined as

$$\mathbf{V}=\arg\min\log(\mathbf{A}^H\mathbf{P}_{\hat{\mathbf{A}}}^{\perp}\mathbf{A}) \tag{30}$$

where $\mathbf{A}=[\mathbf{A}(\alpha)\ \mathbf{A}(\beta)]^T$, $\mathbf{P}_{\hat{\mathbf{A}}}^{\perp}=\mathbf{I}_{2M}-\hat{\mathbf{A}}\hat{\mathbf{A}}^{+}$ represents the projection matrix orthogonal to the spanning space of $\hat{\mathbf{A}}$, and $\hat{\mathbf{A}}=[\mathbf{A}(\hat{\alpha})\ \mathbf{A}(\hat{\beta})]^T$ is the estimation of the direction matrix constructed from the estimated values obtained in (28) and (29). Arbitrarily fixing one of the estimated values can obtain another estimated value paired with it. Might as well make the estimated value $\cos\hat{\alpha}_k$ fixed,

then $\cos\hat{\beta}_k$ has $K!$ kinds of combinations. The combination with the minimum value calculated in (30) is the correct pairing. Then the estimated values of azimuth and elevation can be obtained as

$$\hat{\theta}_k = \arctan(\cos\hat{\beta}_i/\cos\hat{\alpha}_k) \tag{31}$$

$$\hat{\phi}_k = \arcsin(\cos^2\hat{\alpha}_k + \cos^2\hat{\beta}_i)^{1/2} \tag{32}$$

where $\cos\hat{\beta}_i\,(i = 1, \cdots, K)$ is the ith element that matches the kth $\cos\hat{\alpha}_k$.

4. PERFORMANCE ANALYSIS

4.1. Complexity Analysis

This section will calculate and compare the computational complexity of RD-MUSIC and root-RD-MUSIC proposed in this paper with the known RC-MUSIC [21] and 2D-MUSIC algorithm under L-shaped uniform array according to the previous analysis and [11, 13, 21].

The computation of 2D-MUSIC algorithm is mainly concentrated in three parts: 1) calculating the covariance matrix needs $O\{(2M-1)^2L\}$; 2) EVD requires $O\{(2M-1)^3\}$; 3) spectral peak search costs $O\{J^2[(2M-1)^2(2M-1-K)]\}$. J is the number of searching grids, i.e., the product of the search range and the reciprocal of the search step.

The complexity of RC-MUSIC algorithm also focuses on the above three parts, which are $O\{(2M^2L\}$, $O\{2M^3\}$, and $O\{(J_u + KJ_v)[(2M-1)^2(2M-1-K)]\}$, respectively, so does the proposed RD-MUSIC algorithm, which are as follows: $O\{M^2L + (2M-1)^2L\}$, $O\{M^3 + (2M-1)^3\}$, and $O\{J_u[M^2(M-K)] + KJ_v[(2M-1)^2(2M-1-K)]\}$. J_u and J_v are the search grids of u and v, respectively.

Finally, the calculation complexity of root-RD-MUSIC algorithm is slightly different from the first two algorithms. The first two parts are still calculating covariance matrix and EVD, and the complexity is $O\{2M^2L+2M^3\}$; the third part is polynomial root finding, which needs $O\{2(M^2(M-K+1)+M)+(2(M-1))^3\}$; the last part is the angle pairing, and the complexity is $O\{K![(2M)^2K+2MK^2+(2M)^3]\}$. Notably, the complexity of finding the root of polynomial is the third power of the highest order number of polynomial.

The total computational complexity of different algorithms is shown in Table 1. Further, Fig. 2 shows the complexity comparison of the above algorithms under different M values, where $K = 2$, $L = 100$. It clearly demonstrates that the complexity of the proposed RD-MUSIC algorithm is far less than that of the 2D-MUSIC algorithm and improved compared with RC-MUSIC algorithm. Moreover, the complexity of the root-RD-MUSIC algorithm is lower than that of the proposed RD-MUSIC algorithm, which proves that the dimensional reduction algorithms proposed in this paper have greatly improved the computational efficiency.

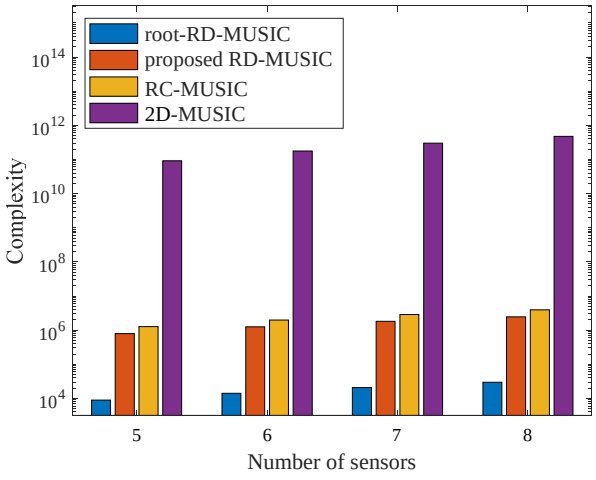

Figure 2. Comparison of the computational complexity with different M.

Table 1. Computational complexity of different algorithms.

Algorithm	Computational complexity
Proposed	$O\{M^2L+(2M-1)^2L+M^3+(2M-1)^3+J_u$
RD-MUSIC	$[M^2(M-K)]+KJ_v[(2M-1)^2(2M-1-K)]\}$
Root-RD-MUSIC	$O\{2(M^2(M-K+L+1)+8(M-1)^3+M)$ $+K![(2M)^2K+2MK^2+(2M)^3]\}$
RC-MUSIC	$O\{2M^2L+2M^3+(J_u+KJ_v)[(2M-1)^2(2M-1-K)]\}$
2D-MUSIC	$O\{(2M-1)^2L+(2M-1)^3+J^2[(2M-1)^2(2M-1-K)]\}$

4.2. Cramer-Rao Bound

In the field of parameter estimation, scholars put forward Cramer-Rao bound (CRB) as a criterion to compare the estimation performance. CRB is the lower limit of the variance of unbiased estimator, that is, the variance of estimator can only be infinitely close to CRB but not lower than this limit. The derivation of CRB in L-shaped uniform array is given below to evaluate the 2D DOA estimation performance of the algorithms mentioned in this paper.

Denote the matrix $\mathbf{A}$ in (30) as $\mathbf{A}=[\mathbf{a}_1,\cdots,\mathbf{a}_K]$, and $\mathbf{a}_k$ is the kth column of matrix $\mathbf{A}$. According to [21] and [23], the CRB of an L-shaped uniform array can be expressed as

$$\mathrm{CRB}=\frac{\sigma^2}{2L}\left\{\mathrm{Re}\left[(\mathbf{D}^H\mathbf{\Pi}_{\mathbf{A}}^{\perp}\mathbf{D})\oplus\hat{\mathbf{P}}^T\right]\right\}^{-1} \tag{33}$$

where $\mathbf{D}=\left[\frac{\partial\mathbf{a}_1}{\partial\theta_1},\frac{\partial\mathbf{a}_2}{\partial\theta_2},\cdots,\frac{\partial\mathbf{a}_K}{\partial\theta_K},\frac{\partial\mathbf{a}_1}{\partial\phi_1},\frac{\partial\mathbf{a}_2}{\partial\phi_2},\cdots\frac{\partial\mathbf{a}_K}{\partial\phi_K}\right]$, $\oplus$ is Hadamard product, $\mathbf{\Pi}_{\mathbf{A}}^{\perp}=\mathbf{I}_{2M}-\mathbf{A}(\mathbf{A}^H\mathbf{A})^{-1}\mathbf{A}^H$, $\hat{\mathbf{P}}=\begin{bmatrix}\hat{\mathbf{R}}_S & \hat{\mathbf{R}}_S\\ \hat{\mathbf{R}}_S & \hat{\mathbf{R}}_S\end{bmatrix}$, $\hat{\mathbf{R}}_S=\mathbf{S}(t)\mathbf{S}^H(t)/L$.

5. SIMULATION RESULTS

Assume that there are two mutually independent far-field narrowband signals (i.e., $K=2$), which are incident on the L-shaped array as shown in Fig. 1(a) at 2D angles of $(\theta_1,\phi_1)=(30^\circ,35^\circ)$ and $(\theta_2,\phi_2)=(80^\circ,70^\circ)$. Set the number of sensors as $2M-1$, the spacing between sensors as half wavelength, and the number of search grids as $J=J_u=J_v=9\times10^3$. The number of Monte Carlo experiments is $N=500$, and the root mean square error (RMSE) of 2D DOA estimation can be defined as

$$\mathrm{RMSE}=\frac{1}{K}\sum_{k=1}^{K}\sqrt{\frac{1}{N}\sum_{j=1}^{N}(\hat{\theta}_{k,j}-\theta_k)^2+(\hat{\phi}_{k,j}-\phi_k)^2} \tag{34}$$

where θ_k and ϕ_k are the real values of the azimuth and elevation angles of the target signal, respectively. $\hat{\theta}_{k,j}$ and $\hat{\phi}_{k,j}$ are the estimated values of θ_k and ϕ_k in the jth Monte Carlo experiment.

5.1. Scatter Figures

Figures 3(a) and (b) are scatter diagrams of the angle estimation values obtained through 500 Monte Carlo experiments when the signal-to-noise ratios (SNRs) of the proposed RD-MUSIC and root-RD-MUSIC algorithms are -5 dB and 5 dB, respectively, where $M=8$ and $L=200$. As shown in the figure, it can be seen that both algorithms can effectively estimate the azimuth and elevation angles of the target signal, no matter in low SNR or high SNR. Besides, with the increase of SNR, the accuracy of algorithm estimation is obviously improved, that is, the range of scatter distribution approaches to one point.

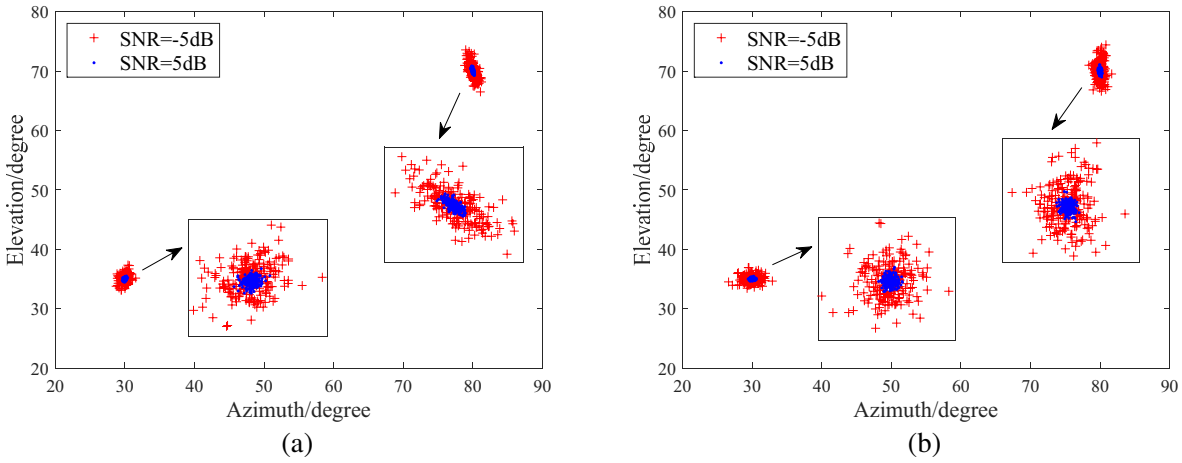

Figure 3. Angle estimation scatter plot, (a) proposed RD-MUSIC, (b) root-RD-MUSIC.

5.2. RMSE Performance Comparison Results versus Snapshot

Figures 4(a) and (b) show the curves of RMSE of the proposed RD-MUSIC and root-RD-MUSIC algorithms changing with the SNR under different snapshot numbers, respectively. Set the number of snapshots L to increase from 100 to 400 at intervals of 100, and the SNR to increase from 0 dB to 25 dB at intervals of 5 dB. The number of sensors is 15, i.e., $M = 8$. It can be clearly seen from the figure that as the SNR and the number of snapshots increase, the RMSE of the 2D angle estimates obtained by the two algorithms decreases, that is, the estimation performance increases.

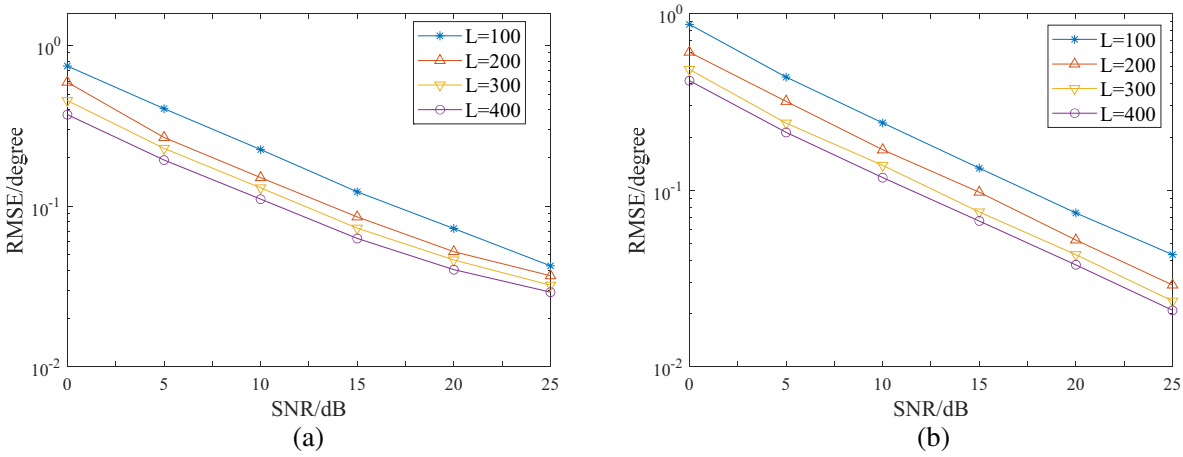

Figure 4. RMSE performance versus snapshot, (a) proposed RD-MUSIC, (b) root-RD-MUSIC.

5.3. RMSE Performance Comparison Results versus Sensor

Figures 5(a) and (b) show the curves of RMSE of the two algorithms proposed in this paper with the change of SNR under different numbers of sensors. Set the value of M to increase from 6 to 10 at intervals of 1, $L = 200$, and the value of SNR is the same as the last experiment. Because the feedbacks given by different sensors are independent of each other, the more the sensors are, the higher the gain of the antenna array may be. It can also be seen from Fig. 5 that under the same SNR, the higher the number of sensors is, the higher the angle estimation accuracy of the algorithm is. However, in practical application, excessive number of sensors will increase cost and computation hugely, so it is enough to select an appropriate value to achieve the required accuracy.

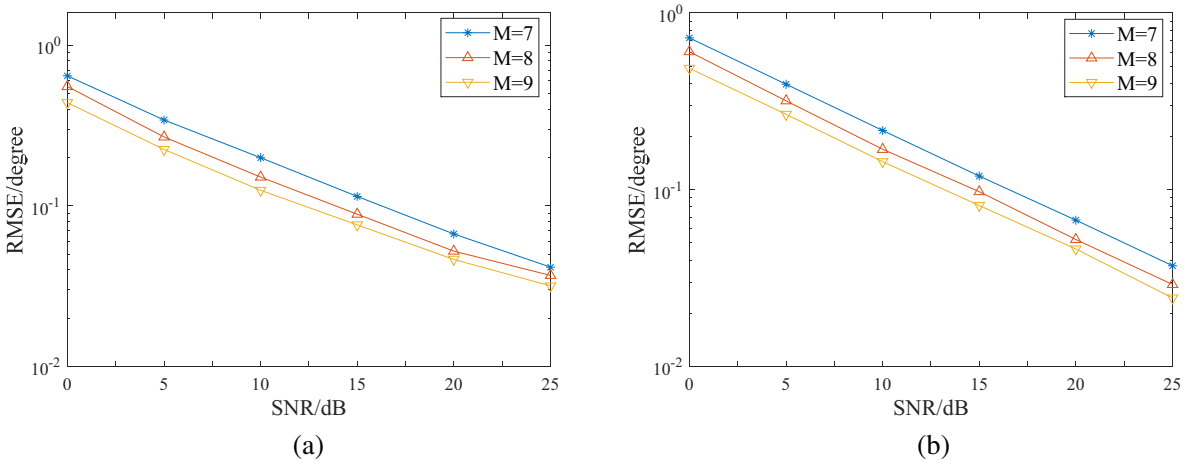

Figure 5. RMSE performance versus sensor, (a) proposed RD-MUSIC, (b) root-RD-MUSIC.

5.4. Estimation Performance Comparison of Different Algorithms

Under L-shaped uniform array, Fig. 6 compares the performance of the proposed RD-MUSIC and root-RD-MUSIC algorithms with 2D-MUSIC algorithm, RC-MUSIC algorithm, and known RD-MUSIC algorithm. In Fig. 6(a), $M = 8$, $L = 200$, SNR increases from -5 dB to 20 dB at intervals of 5 dB. And $M = 8$, $L = 50, 100, 200, 300, 400, 500$, SNR $= 10$ dB in Fig. 6(b). As shown in the figure, the decline rate of RMSE of RC-MUSIC algorithm slows down with the increase of SNR and snapshot number. However, the accuracy of angle estimation of the proposed RD-MUSIC algorithm is always close to CRB, which is better than other methods. Secondly, the estimation accuracy of the proposed root-RD-MUSIC algorithm is higher than that of the RD-MUSIC algorithm. At the same time, it has lower computation. Compared with 2D-MUSIC algorithm, although the estimation accuracy is slightly lower, considering the influence of algorithm complexity, the overall performance of root-RD-MUSIC algorithm is still higher than 2D-MUSIC algorithm under appropriate accuracy requirements. Moreover, when SNR is greater than 0 dB and L greater than 100, the estimation accuracy of root-RD-MUSIC is greater than that of RC-MUSIC. It can be seen from Fig. 6(b) that with the increase of snapshot number, RMSE decreases gradually. Considering the positive correlation between snapshot number and algorithm computation, the value of snapshot number is not the larger the better, so it is only necessary to select an appropriate value to achieve the required estimation accuracy.

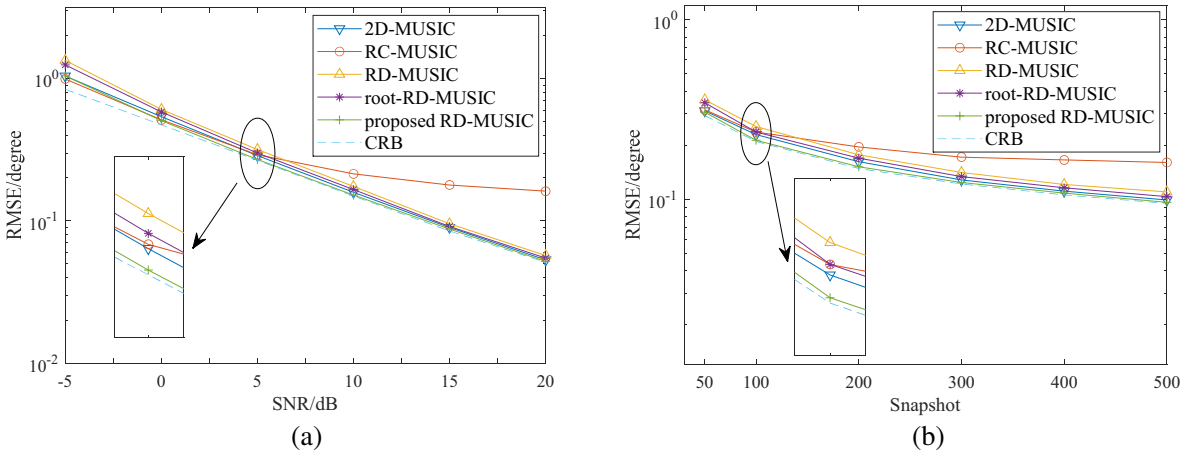

Figure 6. Comparison of RMSE performance of different algorithms, (a) $L = 200$, (b) SNR $= 10$ dB.

6. CONCLUSIONS

In this paper, taking advantage of the structural particularity of L-shaped array in 2D DOA estimation array, a low complexity and high estimation accuracy algorithm which can realize automatic angle pairing is proposed. In order to improve the running efficiency, the proposed algorithms reduce the 2D spectral peak search to 1D search, which greatly reduces the complexity of the algorithm. At the same time, the covariance information of the received data is fully utilized to construct the total noise subspace to estimate the elevation angle, which improves the estimation accuracy and realizes the automatic matching of angles. In order to further reduce the complexity, a polynomial root finding method is proposed instead of 1D spectral peak search. Although the estimation accuracy decreases slightly, the efficiency of the algorithm is significantly improved. In addition, the CRB of L-shape uniform array is deduced in this paper. Finally, the simulation results show that the complexity of this algorithm is much lower than that of 2D-MUSIC algorithm, and the estimation accuracy is higher.

REFERENCES

1. Fulton, C., J. L. Salazar, Y. Zhang, et al., "Cylindrical polarimetric phased array radar: Beamforming and calibration for weather applications," *IEEE Transactions on Geoscience and Remote Sensing*, Vol. 55, No. 5, 2827–2841, May 2017.
2. Jiang, J., Z. Sun, F. Duan, et al., "Disguised bionic sonar signal waveform design with its possible camouflage application strategy for underwater sensor platforms," *IEEE Sensors Journal*, Vol. 18, No. 20, 8436–8449, Oct. 2018.
3. Yazdani, S., S. Fallet, and J.-M. Vesin, "A novel short-term event extraction algorithm for biomedical signals," *IEEE Transactions on Biomedical Engineering*, Vol. 65, No. 4, 754–762, Apr. 2018.
4. Zou, D., W. Meng, S. Han, K. He, and Z. Zhang, "Toward ubiquitous LBS: Multi-radio localization and seamless positioning," *IEEE Wireless Communications*, Vol. 23, No. 6, 107–113, Dec. 2016.
5. Schmidt, R., "Multiple emitter location and signal parameter estimation," *IEEE Transactions on Antennas and Propagation*, Vol. 34, No. 3, 276–280, Mar. 1986.
6. Roy, R. and T. Kailath, "ESPRIT-estimation of signal parameters via rotational invariance techniques," *IEEE Transactions on Acoustics, Speech, and Signal Processing*, Vol. 37, No. 7, 984–995, Jul. 1989.
7. Sun, F., P. Lan, and G. Zhang, "Reduced dimension based two-dimensional DOA estimation with full DOFs for generalized co-prime planar arrays," *Sensors*, Vol. 18, No. 6, 1–10, 2018.
8. Wu, Y. T., G. S. Liao, and H. C. So, "A fast algorithm for 2-D direction-of-arrival estimation," *Signal Processing*, Vol. 83, No. 8, 1827–1831, 2003.
9. Strobach, P, "Two-dimensional equirotational stack subspace fitting with an application to uniform rectangular arrays and ESPRIT," *IEEE Transactions on Signal Processing*, Vol. 48, No. 7, 1902–1914, Jul. 2000.
10. Goossens, R. and H. Rogier, "A hybrid UCA-RARE/root-MUSIC approach for 2-D direction of arrival estimation in uniform circular arrays in the presence of mutual coupling," *IEEE Transactions on Antennas and Propagation*, Vol. 55, No. 3, 841–849, Mar. 2007.
11. Sun, F., P. Lan, and G. Zhang, "Reduced dimension based two-dimensional DOA estimation with full DOFs for generalized co-prime planar arrays," *Sensors*, Vol. 18, No. 6, 1725–1725, 2018.
12. Shi, F., "Two dimensional direction-of-arrival estimation using compressive measurements," *IEEE Access*, Vol. 7, 20863–20868, 2019.
13. Zhao, C., X. Mao, M. Chen, and C. Yu, "Continuous approximation based dimension-reduced estimation for arbitrary sampling," *IEEE Signal Processing Letters*, Vol. 27, 1080–1084, 2020.
14. Xiong, X., M. Zhang, H. Shi, et al., "SBL-based 2-D DOA estimation for L-shaped array with unknown mutual coupling," *IEEE Access*, Vol. 9, 70071–70079, May 2021.

15. Zhang, Y., Y. Sun, G. Zhang, X. Wang, and Y. Tao, "Crosscorrelation and DOA estimation for L-shaped array via decoupled atomic norm minimization," *Wireless Communications and Mobile Computing*, Mar. 2021.
16. Hua, Y., T. K. Sarkar, and D. D. Weiner, "An L-shaped array for estimating 2-D directions of wave arrival," *IEEE Transactions on Antennas and Propagation*, Vol. 39, No. 2, 143–146, Feb. 1991.
17. Tayem, N. and H. M. Kwon, "L-shape 2-dimensional arrival angle estimation with propagator method," *IEEE Transactions on Antennas and Propagation*, Vol. 53, No. 5, 1622–1630, May 2005.
18. Shu, T., X. Liu, and J. Lu, "Comments on 'L-shape 2-dimensional arrival angle estimation with propagator method'," *IEEE Transactions on Antennas and Propagation*, Vol. 56, No. 5, 1502–1503, 2008.
19. Liang, J. and D. Liu, "Joint elevation and azimuth direction finding using L-shaped array," *IEEE Transactions on Antennas and Propagation*, Vol. 58, No. 6, 2136–2141, Jun. 2010.
20. Gu, J. and P. Wei, "Joint SVD of two cross-correlation matrices to achieve automatic pairing in 2-D angle estimation problems," *IEEE Antennas and Wireless Propagation Letters*, Vol. 6, 553–556, 2007.
21. Gong, P., X. Zhang, and W. Zheng, "Unfolded coprime L-shaped arrays for two-dimensional direction of arrival estimation," *International Journal of Electronics*, Vol. 105, No. 9, 1501–1519, 2018.
22. Zhang, Z., Y. Guo, Y. Huang, and P. Zhang, "A 2-D DOA estimation method with reduced complexity in unfolded coprime L-shaped array," *IEEE Systems Journal*, Vol. 15, No. 1, 407–410, Mar. 2021.
23. Tao, H., J. Xin, J. Wang, N. Zheng, and A. Sano, "Two-dimensional direction estimation for a mixture of noncoherent and coherent signals," *IEEE Transactions on Signal Processing*, Vol. 63, No. 2, 318–333, Jan. 2015.